

Gaussian Process Manifold Interpolation for Probabilistic Atrial Activation Maps and Uncertain Conduction Velocity

Supplementary Material

Sam Coveney¹, Cesare Corrado², Caroline H Roney²,
Daniel O'Hare², Steven E Williams², Mark D O'Neill²,
Steven A Niederer², Richard H Clayton¹,
Jeremy E Oakley³, and Richard D Wilkinson³

April 20, 2020

1: Insigneo Institute for *in-silico* Medicine, University of Sheffield, Sheffield, UK.

2: Division of Imaging Sciences and Biomedical Engineering, King's College London, UK.

3: School of Mathematics and Statistics, University of Sheffield, UK.

* E-mail: s.coveney@sheffield.ac.uk

1 Data collection

Patient 1: Data were obtained as part of a study involving patients with paroxysmal atrial fibrillation and undergoing first-time atrial fibrillation ablation. Ethical approval was granted by the National Research Ethics Service (10/H0802/77). Following femoral access and trans-septal puncture, two 8.5 French SR0 long sheaths and a PentaRay mapping catheter (Biosense Webster, CA, 1mm electrode size, 4-4-4mm spacing) were advanced into the left atrium. Decapole (St Jude Medical, MN) and pentapole (Bard Electrophysiology, MA) catheters were positioned in the coronary sinus (CS) and high right atrium (HRA), respectively. An S1-S2 programmed pacing protocol was applied, consisting of a 2-beat drivetrain with a cycle length S1=470 ms followed by a single premature extra stimulus S2<S1. The S1-S2 interval was reduced continuously and without operator interference from 343 ms to 200 ms (or loss of capture) by reducing the current S1-S2 interval by 2% of its value (rounded to nearest ms). All pacing stimuli were delivered at a voltage of at least twice threshold and with a pulse width of 2 ms, from either the CS or HRA. Bipolar electrograms (EGMs) were recorded at a sampling rate of 4 kHz using the 10 electrodes of the PentaRay catheter for each S1-S2 interval. The catheter was then moved to another location on the left atrial endocardium, and the process repeated for up to 15 locations. For each S1-S2 interval, we discarded any EGM traces not containing a discernible activation complex. We obtained left atrial anatomies during the clinical procedures using an electro-anatomical mapping system (St Jude Velocity).

Patient 2: Data were collected as part of routine clinical care for first-time pulmonary vein isolation to treat persistent atrial fibrillation. Ethical approval was granted for retrospective data analysis (REC number 18/HRA/0083). Prior to radiofrequency ablation, left atrial geometry and a paced map were obtained using an Electroanatomical mapping system (CARTO3, Biosense Webster, USA) during constant pacing at a cycle length of 500ms from the proximal (9,10) dipoles of a decapolar catheter positioned in the coronary sinus (CS). Endocardial contact points were acquired using a circular mapping catheter (Lasso 2515; Biosense Webster, USA) introduced to the left atrium via transseptal access.

2 Mesh extension

In order to remove the effects of the Laplacian boundary conditions from the interpolation on the atrial mesh, we extend the mesh with elements as in Figure 1. This does not change the mesh topology, and the shortest distance between points on the original mesh is almost completely unchanged (with small exceptions caused by non-planar clipping of the clinical mesh to produce the holes in the interpolation mesh; for planar or convex edges, the shortest distances would be completely unchanged).

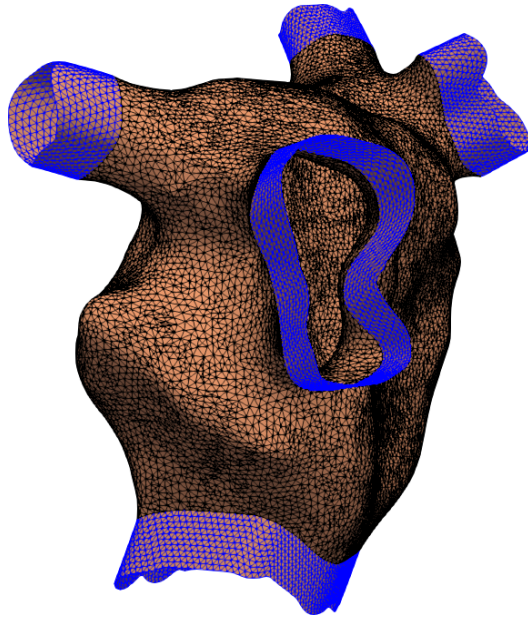


Figure 1: Mesh extension for Patient 2.

The algorithm is as follows. For each hole in the mesh (e.g. mitral valve), the vertices belonging to the ‘edge’ describing this hole are identified (face edges at the mesh edge belong to one face only; this can be used to identify vertices on the mesh edges). These vertex coordinates are used to fit a plane, and the plane normal \vec{n} sign is adjusted such that \vec{n} points away from the mesh centre of mass. Vector \vec{n} points in the direction that layers of elements will be added. Then, starting on any vertex in the edge and proceeding either clockwise or anti-clockwise until all edge vertices have been considered, the following is done:

1. calculate the centre \mathbf{x}_p between current vertex \mathbf{x}_i and neighbouring vertex \mathbf{x}_j
2. add a new vertex at position $\mathbf{x}_n = \mathbf{x}_p + \vec{n} \times |\mathbf{x}_j - \mathbf{x}_i| \tan(60 \text{ deg})/2$
3. append this new vertex \mathbf{x}_n to the list of all vertices
4. append a new element connecting $\mathbf{x}_i, \mathbf{x}_j, \mathbf{x}_n$ to the list of all elements

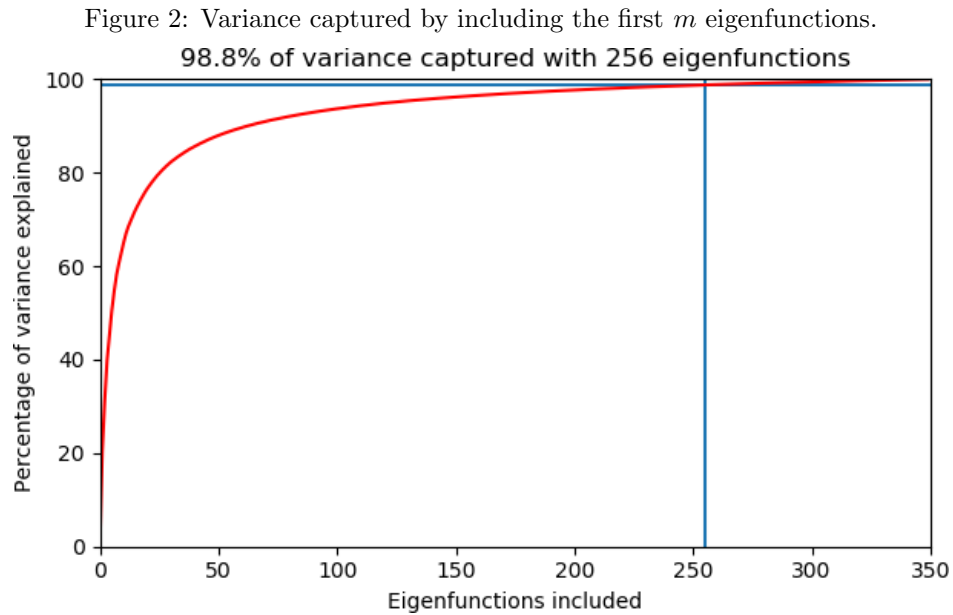
Now the edge will look like the teeth of a saw. New elements must be added to the list of all elements that connect the newly created vertices to each other, and to the original vertex nearest both of them. This concludes the creation of a single layer of new elements. This process can be repeated to build up sufficient layers to prevent the boundary conditions from producing artefacts in the interpolation (the plane normal vectors can be recalculated for each layer, or the original vector used for all layers).

3 Explained Variance

The percentage of variance captured by the first m basis functions can be calculated as

$$EV_m = 100 \times \frac{\sum_{j=1}^m S(\sqrt{\lambda_j})}{\sum_{j=1}^M S(\sqrt{\lambda_j})} \quad \text{where} \quad 1 \leq m \leq M \quad (1)$$

where S is the kernel spectral density evaluated at the square root of the eigenvalue λ_j (kernel hyperparameters have been optimized). Figure 2 shows, for the model fit of the virtual patient with 1000 noisy observations and $M = 350$ basis functions, that the first 256 eigenfunctions capture 98.8% of the variance. Therefore 256 eigenfunctions are more than sufficient for LAT interpolation.



4 Simulation Parameters

Figure 3 shows the parameter values used for simulation of the virtual patient. The parameter values are down-sampled to nodes for visualization purposes. The τ parameter units are milliseconds, and the conductivity units are in cm^2/s . The CARP simulation files can be found at [1].

References

- [1] S Coveney *et al.* Virtual Patient CARP simulation, <https://doi.org/10.5281/zenodo.3755809> (2020)

Figure 3: Parameter values for the simulation (virtual patient).

